An extended chiral surface coordination network based on Ag_7-clusters

Katrine L. Svane[1,a)], Mahdi S. Baviloliaei[2], Bjørk Hammer[1] and Lars Diekhöner[2,b)]

[1]*iNANO, Department of Physics and Astronomy, Aarhus University, Aarhus, 8000 Aarhus C, Denmark*

[2]*Department of Materials and Production, Aalborg University, 9220 Aalborg, Denmark*

We present an extended metal-coordinated structure obtained by deposition of trimesic acid (TMA) onto the Ag(111) surface under UHV conditions followed by annealing to 510 K. Scanning tunneling microscopy and density functional theory calculations reveal the structure to consist of metal clusters containing seven Ag atoms each, coordinated by six dehydrogenated TMA molecules. The molecules are asymmetrically arranged, resulting in a chiral structure. The calculations confirm that this structure has a lower free energy under the experimental conditions than the hydrogen-bonded structures observed after annealing at lower temperatures. We show that the formation of such large metal clusters is possible due to the low adatom formation energy on silver and the relatively strong Ag-O bond in combination with a good lattice match between the structure and the Ag surface.

I. INTRODUCTION

Self-assembly of surface coordination networks presents a tractable way to distribute equally sized metal centres evenly on a surface[1]. Small metal clusters have been shown to have unique properties, exemplified by the catalytic activity of gold nanoclusters[2] or the metal centers in three-dimensional metal-organic frameworks[3]. A few examples also exist of two-dimensional surface coordination networks where the exposed metal clusters have catalytic[4] or magnetic[5,6] properties. In addition the metal-organic units sometimes exhibit interesting chiral effects, e.g. induced by asymmetric binding motifs between the organic molecules and the central metal atom or cluster[1,7–11].

Here we report on the formation of an extended metal-coordinated structure upon deposition of trimesic acid (TMA) onto the Ag(111) surface. The self-assembly of TMA on Ag(111) has previously been studied and two different structures were found; a hydrogen bonded honeycomb network, that was observed upon room temperature adsorption and a more densely packed structure emerging after annealing to 420 K, which was shown to consist of partially dehydrogenated TMA molecules[12–14]. Adatoms of Ag were not observed in either of these structures. We likewise observe these two hydrogen-bonded structures in our experiments, but in addition we identify a different structure upon deposition of TMA at room temperature followed by annealing to a higher temperature of 480-510 K. The same structure has recently been reported, and the self-assembly and dehydrogenation of TMA was investigated by Scanning tunneling microscopy (STM), photo emission and gas-phase DFT calculations, i.e. without taking the surface or metal coordination into account. Speculations about a metal center were

[a)] Current affiliation: Department of Energy Conversion and Storage, Danish Technical University, DK-2800 Kgs. Lyngby, Denmark, [b)] Author to whom correspondence should be addressed. Email: ld@nano.aau.dk

presented, although the exact composition of the central cluster remained inconclusive.[15] Here we use STM experiments and density functional theory (DFT) calculations to reveal that the structure consists of Ag_7-clusters connected by dehydrogenated TMA molecules.

Most previous studies of metal-coordinated structures have revealed small metal centers consisting of at most three adatoms[8,11,16–20], but larger Au clusters have been stabilized by fullerene molecules[21,22]. Relatively large Fe clusters were also observed on the calcite surface, although the exact size of these clusters was not determined[23]. The observed coordination motif is thus unusual because of the large size of the exposed metal clusters. Furthermore, silver has only been reported to form surface coordination structures with reactive ligands containing cyano groups[20] or surface radicals formed by dehalogenation[24,25]. Our DFT calculations allow us to pinpoint some properties of the combined TMA-Ag system, which makes the formation of this structure possible.

II. METHODS

All experiments have been performed under ultra-high-vacuum (UHV) conditions (base pressure of $1x10^{-10}$ mbar). The surface was cleaned by Ne sputtering and annealing to 800 K. TMA (98%, Alfa Aesar) molecules were evaporated from a Knudsen type evaporator onto Ag(111) at room temperature. All STM measurements have been performed at room temperature. The bias voltages *U* are for the tip. The sample is grounded.

DFT calculations were performed using the grid-based projector augmented wave (GPAW)[26,27] software and the ASE interface[28]. In GPAW the wavefunctions and density are represented on a real-space grid, and convergence is determined by the distance between the grid-points. Here we use a value of 0.18Å. All reported energies are calculated using the optB88-vdW[29] functional to describe the exchange and correlation, however some initial screenings were performed using the M06-L meta-GGA functional (for reasons of speed),[30] including the mapping of the potential energy surface for one TMA molecule interacting with an Ag_7 cluster. The two functionals have previously been shown to give similar results for interactions between organic molecules on surfaces, but somewhat different adsorption energies.[31] The optimum lattice constant for the respective functionals (4.19Å (optB88-vdW) and 4.16Å (M06-L), exp. 4.09Å[32]) was used for the silver. The surface was modelled by a two layer slab for initial screenings and further relaxed on a four layer slab for final energies, in all cases keeping the bottom layer fixed during relaxation. Periodic boundary conditions were used in the x- and y-directions while the z-direction was non-periodic with a minimum of 6 Å of vacuum between the atoms and the cell boundary. The honeycomb structure and the partially dehydrogenated close-packed structure were optimised using 2x2 **k**-points, while the metal-coordinated structure was optimised

using 4x4 **k**-points. All structures were relaxed until the forces on individual atoms were below 0.025 eV/Å (0.05 eV/Å for initial screenings).

III. RESULTS

A. STM experiments

Large scale STM images of the structures obtained after room temperature deposition followed by annealing to 480K and 510K are shown in Figure 1a and b, respectively. The molecules form extended domains on the surface, however bare areas (upper left and right part of Figure 1a) between the covered areas suggest that the large domain size is not due to high coverage, but results from an attractive interaction between the molecules.

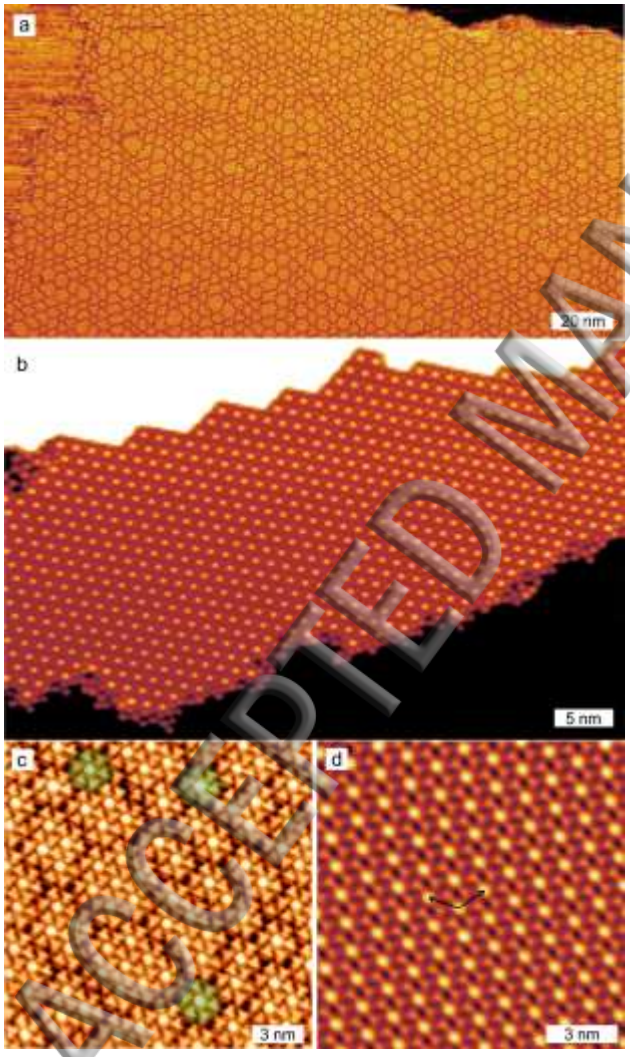

FIG 1 a) STM image (200 x 106 nm, *U*=-0.5V *I*=0.4nA) showing the metal-coordinated TMA structure obtained after annealing to 480K extending over a large area of the surface and b) STM image of a large area of the surface covered by the periodic metal-organic framework obtained after annealing to 510K (56 x 36 nm). The bright and dark areas are clean Ag areas. c) Close-up image of the structure

This manuscript was accepted by J. Chem. Phys. Click here to see the version of record.

with isolated units containing a single metal cluster (some of them coloured green) (18 x 18 nm, *U*=-0.7V *I*=0.4nA). d) Periodic structure observed after further annealing (14 x 14 nm, *U*=-1V *I*=0,1nA), with the unit cell vectors indicated by black arrows.

More detailed images (Figure 1c and d) reveal a structural motif consisting of a central bright protrusion surrounded by 6 triangular shaped units identified as the TMA molecules, which are known to be imaged triangular by STM[12–14,33,34]. The central protrusion is attributed to Ag adatoms, which can evaporate from step edges at the experimental temperatures (the detachment barrier is calculated/measured to be 0.63 eV/ 0.71 eV[35,36]). After annealing to 480K some of these flower-like structures are isolated (green color in Figure 1c) while others are connected by sharing of TMA molecules in small patches of 3-5 nm in width. Annealing at slightly higher temperatures (510 K) completes the connection such that a regular structure appears with large domain size (only limited by the width of the Ag(111) terraces) (Figure 1b and 1d). We thus interpret the structure in Figure 1a and c as an intermediate in the formation of the extended periodic structure in Figure 1b and d. The dimension of the unit cell marked in Figure 1d (and also in Figure 3h, where it is better seen) is measured to be 13.6±0.2 Å and the orientation with respect to the Ag[1-10] direction is determined to be ±(14±3°). The roughening of Ag(111) step edges upon annealing seen in Figure 1b (the upper bright part of the image is an upper terrace of clean Ag) confirms, that silver atoms at step sites have been mobile during annealing. We note that, at the temperature where the extended structure have been formed, we already observe a significant reduction in molecular coverage. The rate of formation is thus in direct competition with desorption of TMA from the surface. This is emphasized by the fact, that increasing the annealing temperature by just a few tens of degrees destroys the structure and leaves a surface free of TMA and otherwise clean, but with step edges that are somewhat rough.

In Figure 2a we show an STM image of a single Ag_xTMA_6 unit. The superimposed molecular models illustrate that the TMA molecules are oriented at an angle $\alpha = 22°(\pm 3°)$, with respect to the axis from the center of the molecule to the molecule on the opposite side of the metal cluster. This asymmetric bond to the metal cluster leads to the existence of two chiral forms of the structure (labeled R and S)[7], shown in Figure 2a and 2b, respectively. A model of the R-structure is shown in Figure 2c for comparison. The procedure to obtain this model will be described in section III B. Both chiralities are observed on the surface, but each large domain contains only one of the two. In Appendix A (Figure 6) we show a S-type domain (R-type domains are shown in Figure 1). Surprisingly, it is not only the extended periodic structure in Figure 1b and d, but also the large areas of disconnected patches in Figure 1a and c that contains only one of the two chiral forms. This requires an interaction between the patches mediating the chiral organization, even when there appears to be a separation between them. We cannot determine the nature of this interaction but speculate that it could be hydrogen bonds between intact carboxylic acid groups or single adatoms that appear invisible in the STM images. We note, that we occasionally have observed a few units with opposite chirality, if these have been well separated and isolated within the domain (c.f. Appendix A, Figure 7).

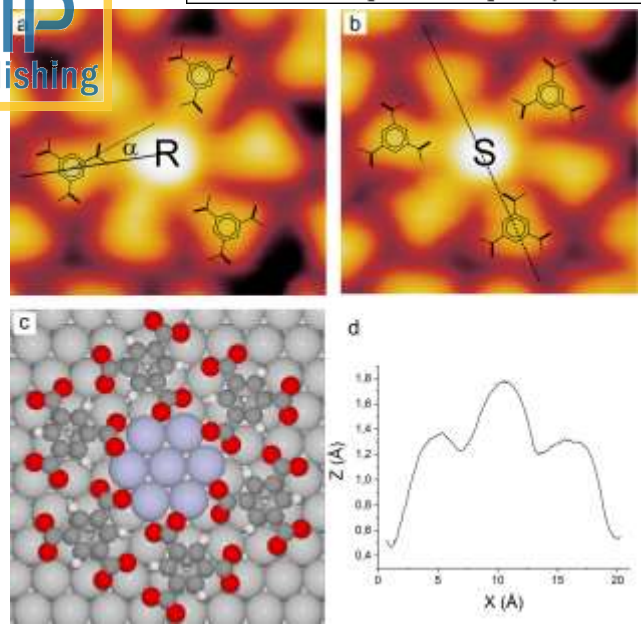

FIG 2: a) STM image of a single Ag_7TMA_6 (2 x 2 nm) with superimposed molecular models to illustrate the chirality (R-type shown, angle α=22°), b) STM image of a single Ag_7TMA_6 unit (S-type) c) Atomic model of the structure (R-type), based on the DFT calculations, and d) Line scan across the Ag_7TMA_6 (dashed line shown in b).

On Cu(100) similar flower-like structures consisting of 4 TMA molecules and single metal atom centers of Cu[37] or Fe[11], respectively, have been observed. The angle α for Cu-TMA_4 was minimal and chirality was not discussed, whereas for Fe-TMA_4 both R and S enantiomers were seen with α=22,5°. In both experiments the central protrusion was significantly smaller than observed here, and was assigned to a single atom center

B. Density functional theory based structure determination

1. Dehydrogenation state

To determine the atomic structure of the metal-coordinated structure we firstly considered the dehydrogenation state of the TMA molecule. The most stable adsorption configurations of the intact and dehydrogenated molecules are identified by DFT calculations and the resulting structures are shown in Figure 3a-b. The adsorption enthalpies are given in the bottom of the images (grey numbers in parenthesis) together with the adsorption free energies (black numbers), which are calculated assuming a pressure of 10^{-7} Pa and a temperature of 298 K, following the procedure described in ref. 38. This approach accounts for the changes in entropy and zero point energy arising when two O-H groups are dehydrogenated to form one hydrogen molecule which desorbs from the surface, but neglects contributions from vibrations in other parts of the molecule. The adsorption free energies of the isolated molecules are compared to the calculated free energies of the self-assembled structures obtained at different annealing temperatures in Figure 3. The procedure for obtaining these structures are described in the following sections.

The lower free energy of the dehydrogenated molecule implies that dehydrogenation of all three carboxylic acid groups of TMA is thermodynamically favorable under the experimental conditions. The enthalpy increases upon dehydrogenation, but the reaction is driven by the high entropy of molecular hydrogen at low pressure, as also found in previous studies[39]. Experimentally only partial dehydrogenation of TMA on Ag(111) was observed at 420K[12], suggesting that the reaction has a high energy barrier. The level of dehydrogenation in the annealed [illegible] perature[40] and the experiments performed in Ref. 15 indeed [illegible]g that the molecules in the extended

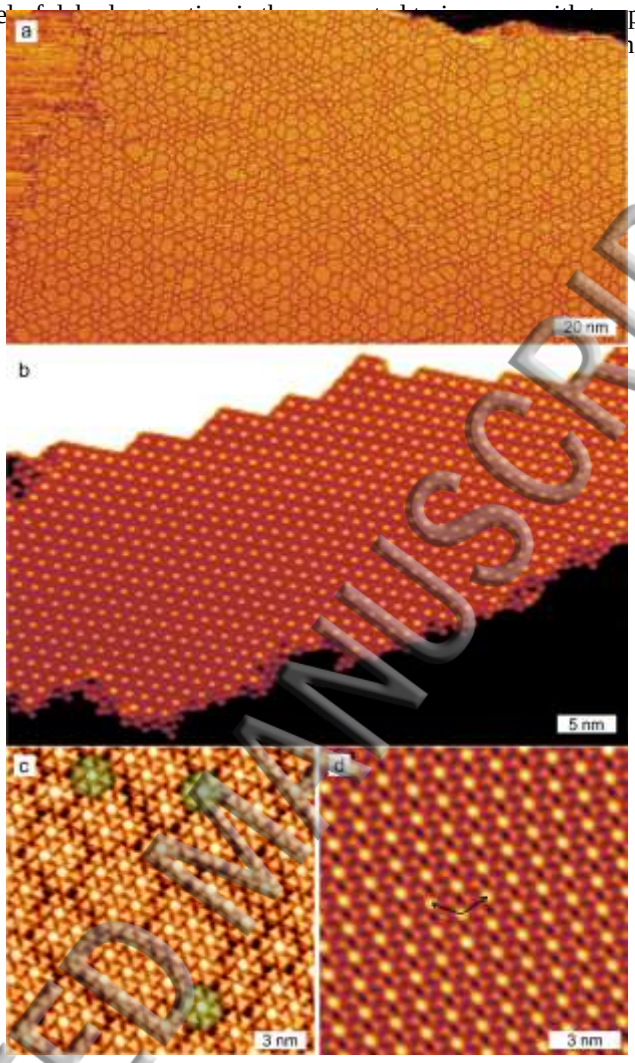

metal-coordinated structure (
FIG 1 b and d) are completely dehydrogenated.

2. Metal-coordinated structure

To consider the possible numbers of adatoms in the metal center we choose a unit cell commensurate with the Ag substrate and in close agreement with the experimentally determined unit cell parameters (|**a**|=|**b**|=13.3 Å and ∠ **a**, Ag[1-10] = 11°, see Table 1 in Appendix B for comparison with experimental values). A configuration where the dehydrogenated TMA molecules are placed around the simplest possible adatom cluster, namely a single adatom, results in very large Ag-O distances of ca. 4.2Å (e. g. compared to the typical Ag-O distance in AgO_2 of 2.05 Å[41]) (c.f. Appendix C for an image of this structure).

Acknowledging the uncertainties in distances determined by STM we tried to move the TMA molecules closer to the adatom (as would be the case if the unit cell was smaller), however this lead to repulsion between the carbonyl groups of neighboring

molecules. We therefore conclude that the clusters must contain more than one Ag atom, which seems reasonable given the large apparent diameter of approximately 6 Å determined from the STM images (see line scan in Figure 2d). The next cluster size consistent with the observed sixfold symmetry and (slightly) hexagonal shape, is a hexagon containing 7 atoms as shown in the model in Figure 2c. A few structures with 3 or 6 adatoms were also considered, but were found to be less stable (c.f. Appendix C). We note that the apparent cluster size in the STM images cannot be directly correlated with the size of the metal cluster in the atomic model, as the attachment of the TMA molecules can affect the local density of states (LDOS). Indeed, our calculations show that the 6 outer Ag atoms are positively charged due to the coordinating TMA molecules.

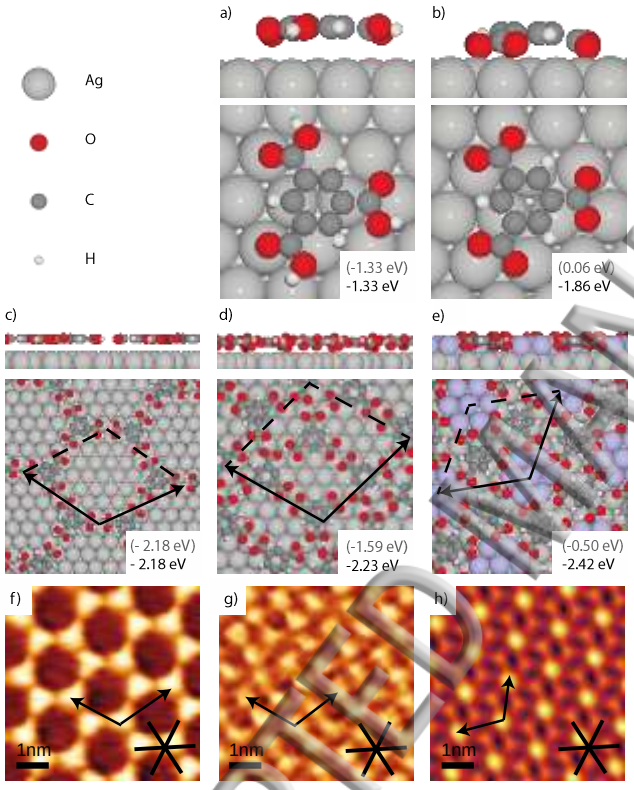

FIG 3 Top and side view of the calculated adsorption configuration of TMA (a) and dehydrogenated TMA (b) as well as optimised structures for the honeycomb phase[a] (c), close packed phase (d) and metal-coordinated structure (e). The free energy per molecule relative to the intact molecule in the gas phase is given in the bottom of each image in black and enthalpies are given in parenthesis in grey. Adatoms are colored differently for clarity. (f-h) shows STM-images of the structures in c-e for comparison (all are sized 6 x 6 nm) and the orientation of the Ag(111) substrate is indicated. Imaging parameters: f: U=-0.61V, I=0.4nA; g: U=0.27V, I=0.4nA, h: U=-0.042V, I=5.7nA.

To determine the periodic structure we firstly identify the most stable adsorption configuration of one dehydrogenated TMA molecule interacting with the Ag_7 adatom cluster on the Ag(111) surface. Following a procedure similar to the one described in ref. [42], we systematically test different orientations of the molecule in intervals of 7.5° as well as different positions of the

[a] We note that the image of the honeycomb structure shown here is not the lowest energy structure as calculated by DFT, but rather the structure that matches the orientation relative to the substrate of the STM image in Figure 3f.

This manuscript was accepted by J. Chem. Phys. Click here to see the version of record.

molecule relative to the center of the adatom. The potential energy surface is three-dimensional, but can be visualised as two-dimensional plots, showing the energy as a function of the position on the surface for a given molecular orientation (c.f. FIG 4a for an example). From these plots the most stable configuration, shown in FIG 4b, is determined. In this configuration the vertical mirror plane of the Ag_7 cluster and the C-C bond direction of the interacting carboxyl group form an angle of 22.5° (α in FIG 4b, corresponding to α in FIG 2a). The molecule makes an asymmetric contact to the cluster with the carboxyl group rotated such that one oxygen atom is bonding towards the surface as well as to an atom of the cluster (O-$Ag_{cluster}$ = 2.4Å) and the other is bonding to the cluster only (O-Ag = 2.2 Å). The single flower shown in FIG 2c is constructed by repeating this configuration symmetrically around the metal cluster and relaxing the structure. The relaxation leads to a small reorientation of the molecule such that the angle α becomes 28°. Finally, the adsorption configuration of a molecule in the single flower fits almost perfectly in the commensurate unit cell with |a|=|b|=13.3 Å and ∠ |a|, Ag[1-10] = 11° and the molecular orientation only changes slightly to α=29° upon relaxation in this unit cell. The periodic structure (Figure 3e, compare with the STM image in FIG 3h) is thus an extension of the most stable adsorption geometry of a single molecule next to a 7-adatom cluster (Figure 4b), slightly distorted to optimize the interaction with neighbouring molecules and match the periodicity of the substrate. The given free energy per molecule (-2.42 eV) includes the energetic cost of adatom formation and is lower than that of the adsorbed isolated molecule after dehydrogenation (-1.86 eV). Here, bulk Ag is used as reference for the adatoms, since the process of moving an atom at a kink site on to the terrace effectively corresponds to reducing the number of bulk atoms by one.

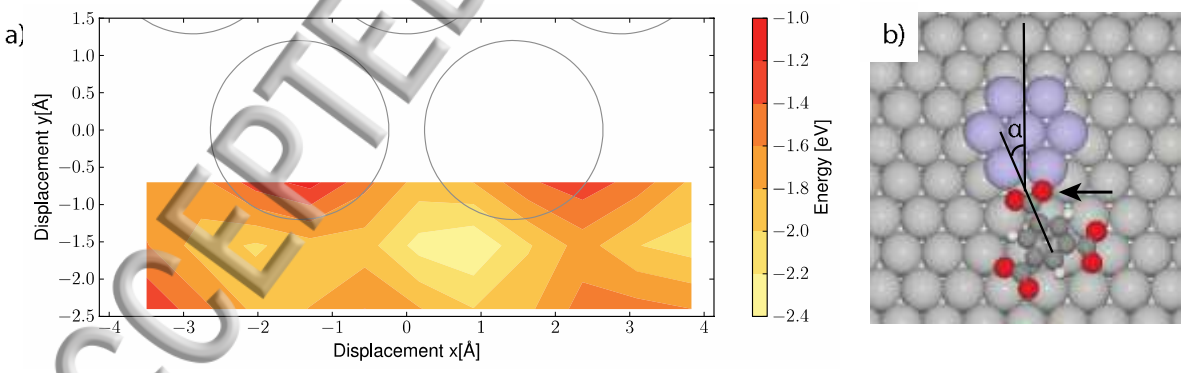

FIG 4 a) Energy map (2 layers of Ag, M06-L functional) showing the adsorption energy when a TMA molecule with α =22.5 is moved along the x- and y- direction. The two circles mark the position of the two lowest Ag atoms in the cluster, and the centre between them is the origin of the coordinate system. The position on the map is the initial position of the oxygen atom of TMA with the highest y-coordinate (marked with an arrow in b). b) Most stable adsorption configuration of a single molecule. The angle with the mirror plane of the metal cluster, α, is indicated.

3. Hydrogen bonded structures

To understand the observed evolution of the TMA structures, we now compare the free energy of the metal-coordinated structure to that of the two structures observed after annealing to 300K and 420K. The structural models of the two latter structures are based on the proposed molecular models in ref. 12. The unit cell size obtained here was compared with our experimental results and adapted to make the structures commensurate with the substrate (c.f. Table 1 in Appendix B).

The unit cell size of the honeycomb structure is measured to be 16.0 ± 0.3 Å in our experiment while the value given by Payer et al. is 17.8 Å (c.f. Table 1 in Appendix B). Because of this uncertainty, the energy of the honeycomb structure is initially calculated in the gas phase for different sizes of the unit cell, leading to the red energy curve shown in FIG **5**a. It is found that a unit cell size of 16.5Å gives the best hydrogen bonding energy, with O-O donor-acceptor distances of 2.6Å. For the Ag(111) surface, the commensurate unit cell that best matches this size has a side length of 16.3 Å and an orientation of 9° with respect to the Ag[1$\bar{1}$0] direction. The molecules are preferentially placed in hollow or bridge sites, as top sites were found to be the least favourable for isolated molecules, leading to the optimized structure shown in FIG **5**b (compare with STM image in FIG 3f). Two larger unit cells matching the parameters measured in ref. 12 were also tested but both resulted in a higher energy (FIG **5**c-d) due to longer hydrogen bonds with O-O distances larger than 3.0 Å. For all three unit cell sizes, the adsorption of the hydrogen bonded structure on the surface led to similar energy gains of 1.0-1.2 eV per molecule as indicated in FIG **5**a.

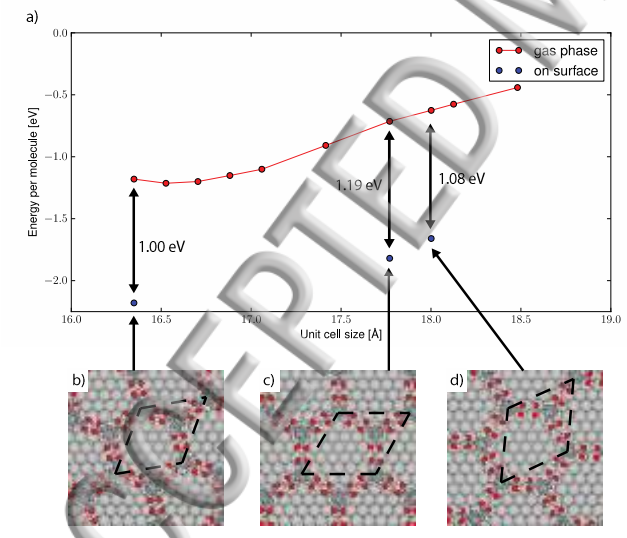

FIG 5 a) Energy of the TMA honeycomb structure in the gas phase as a function of the unit cell vector length (red line) and energy of the structure in the three different commensurate unit cells (blue points) shown in b-d).

The commensurate cell that best matches the parameters for the close-packed structure has unit cell vectors of **a** = 18.0 and **b**

= 18.5Å, ∠**a,b** = 101° and an angle between the Ag[1-10] direction and the **a**-vector of 25° (c.f. Table 1, Appendix B). The initial positions of the molecules are estimated from the structure suggested in ref. 12. Again they are preferentially placed in hollow or bridge sites, but a systematic identification of the best combination of (non-identical) adsorption sites has not been performed.

For the close-packed structure there also exists another unit cell with approximately the right size, but > 10° deviation on the orientation. Modelling the structure in this alternative cell results in a structure which is 0.01 eV lower in energy, however this energy difference is within the uncertainties of the calculations and we have thus given the value obtained in the unit cell that matches the experimental parameters in FIG 3d (compare with STM image in FIG 3g). These findings however indicate that for both the honeycomb and the close-packed structure different registries of the molecules relative to the surface only lead to small differences in energy.

C. Discussion

Comparing the free energies of the three self-assembled structures (FIG 3c-e) the evolution of the TMA structures can be understood. The system gains 0.85 eV per molecule when the isolated molecules (-1.33eV/molecule) form the hydrogen bonded honeycomb structure (-2.18eV/molecule). The energy is lowered by 0.05 eV/molecule when the partially dehydrogenated structure (-2.23 eV/molecule) is formed, and decreases further by 0.19eV/molecule upon formation of the Ag_7 metal-coordinated network (-2.42 eV/molecule), despite the formation of an Ag_7 cluster from the substrate requiring a significant energy (1.91 eV). From our structural optimization and the large extension of the domains seen in the STM images it is clear that the structure has a good lattice matching with the substrate. We therefore investigated the possibility of forming the corresponding structure on gold, which has a similar lattice constant to Ag (Exp: 4.08 vs 4.09 Å[32]) but a higher cohesive energy (Exp: 3.81 vs 2.95 eV[32]), however our results show that the structure cannot be formed on this substrate (c.f. Appendix D for details). Here, the adsorption of isolated intact TMA molecules is more favorable, consistent with previous calculations showing that dehydrogenation of carboxylic acid groups on Au(111) is not favorable[38]. We thus point at the relatively strong Ag-O bond as an important factor for the formation of the metal-coordinated structure.

The distribution of equally sized metal clusters on the surface suggests interesting applications in e.g. catalysis and sensing. For such applications, the properties of the exposed metal atoms are important. Bader charge analysis[43] of the adatom cluster reveals that the six outer atoms carry a positive charge of +0.4e each, while the central atom is almost neutral. The cluster can thus be expected to behave differently to uncoordinated clusters of the same size.

VI. CONCLUSION

In conclusion TMA dehydrogenates completely upon annealing to 510 K and forms extended chiral domains of a metal-coordinated structure based on Ag_7 clusters. DFT calculations show that this structure has a lower free energy per molecule under the experimental conditions than the hydrogen bonded structures observed after annealing to lower temperatures. The formation of these relatively large 7-atom Ag clusters is possible due to the low adatom formation energy on silver and the relatively strong Ag-O bond.

Appendix A: Supplementary STM images

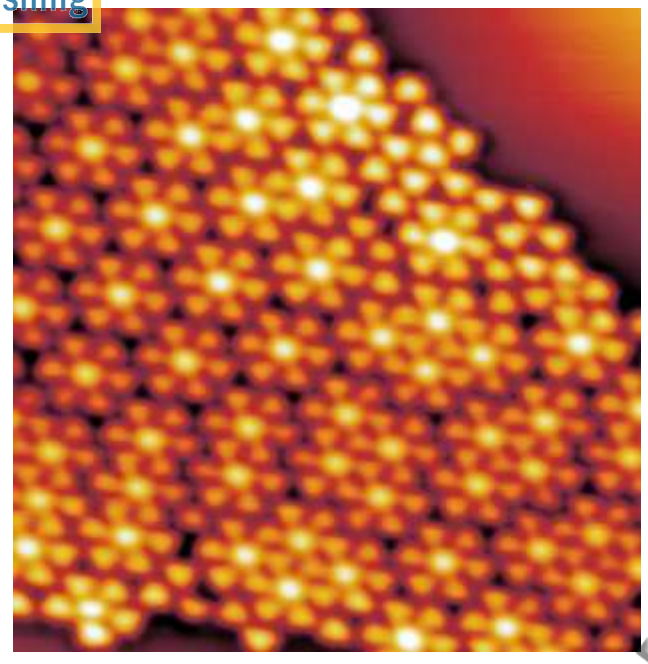

FIG 6: STM image of $Ag_7TMA_6/Ag(111)$ (13 x 13 nm). The chirality is S-type.

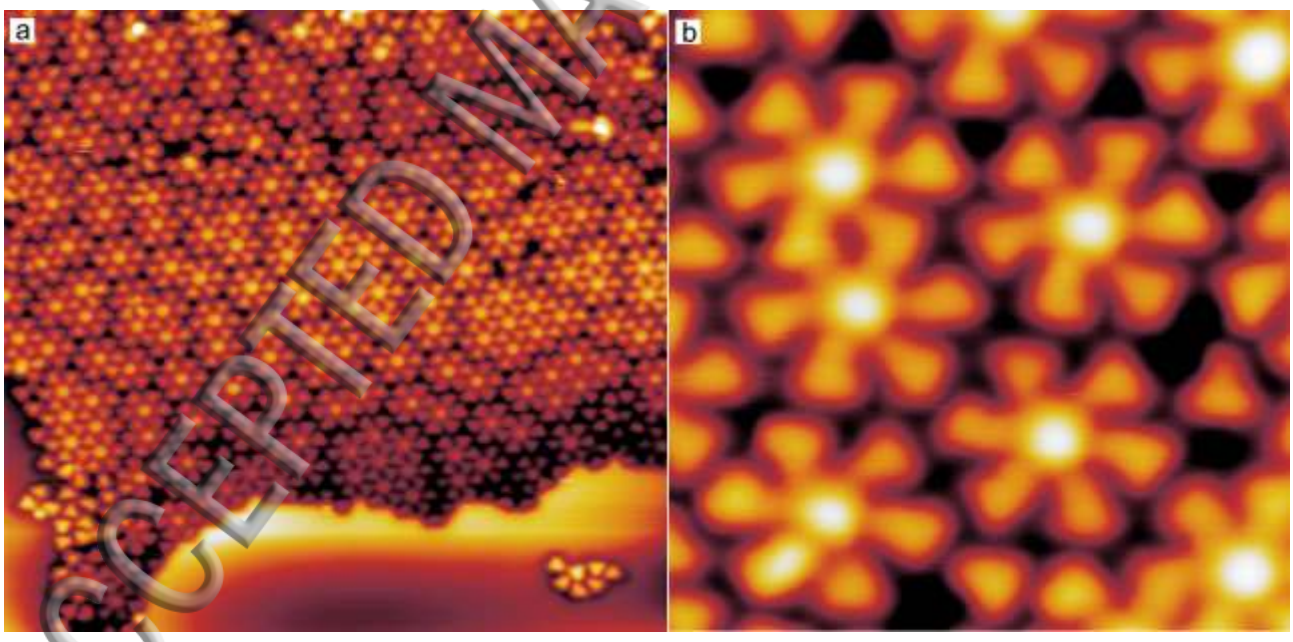

FIG 7: a) STM image of $Ag_7TMA_6/Ag(111)$ (23,4 x 21,6 nm). The chirality is dominantly R-type, with a few units of S-type in the lower left part of the image. b) close-up image showing both R-type and S-type (4,5 x 4,5 nm).

This manuscript was accepted by J. Chem. Phys. Click here to see the version of record.

Appendix B: Comparison of calculated and experimentally determined lattice parameters

Table 1 Comparison of experimental unit cells and unit cell parameters of all investigated DFT cells. The matrix notation for the DFT optimized structures is given with the conventional choice of basis set vectors with an angle between them of 120°.

Structure		$\lvert\mathbf{a}\rvert$ [Å]	$\lvert\mathbf{b}\rvert$ [Å]	$\angle\,\mathbf{a},\mathbf{b}$ [°]	$\angle\,\mathbf{a}$, Ag[1-10] [°]	Figure	Matrix notation
Honeycomb	Exp.[12]	17.8±0.5	17.8±0.5	120	Not given		
	Exp. (this work)	16.0±0.5	16.0±0.5	120	0 and 30±5		
	DFT - small	16.3	16.3	120	9	5b	$\begin{pmatrix} 6 & 1 \\ -1 & 5 \end{pmatrix}$
	DFT - medium	17.8	17.8	120	0	5c	$\begin{pmatrix} 6 & 0 \\ 0 & 6 \end{pmatrix}$
	DFT – large	18.0	18.0	120	25	3c and 5d	$\begin{pmatrix} 4 & -3 \\ 3 & 7 \end{pmatrix}$
Closepacked	Exp.[12]	17.7±0.5	18.7±0.5	102	Not given		
	Exp. (this work)	18.3±0.5	18.4±0.5	103	±(25±5)		
	DFT	18.0	18.5	101	25	3d	$\begin{pmatrix} 7 & 4 \\ -2 & 5 \end{pmatrix}$
	DFT alternative	17.8	18.5	104	0	Not shown	$\begin{pmatrix} 6 & 0 \\ 2 & 7 \end{pmatrix}$
Metal-coordinated	Exp. (this work)	13.6	13.6	120	±(14±3)		
	DFT	13.3	13.3	120	11	3e	$\begin{pmatrix} 5 & 1 \\ -1 & 4 \end{pmatrix}$

Appendix C: Investigated metal clusters with less than 7 adatoms

A structure with only one adatom in the center in a commensurate cell consistent with the experimental parameters is shown in Figure 8. As the oxygens are clearly too far away from the adatom for any significant interaction we conclude that this cluster is too small.

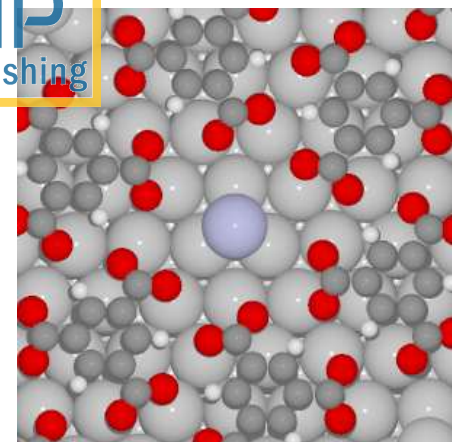

FIG 8: TMA-Ag structure assuming the Ag cluster consists of a single adatom

When investigating the formation of a single Ag_xTMA_6 cluster a few structures containing 3 or 6 adatoms, inspired by the optimized structure with 7 adatoms, were also tested. These structures are shown in Figure 9, and the energy per molecule is compared after relaxation on four layers of Ag to a maximum force of 0.05eV/ Å. Based on these results we decided to focus on the structure with 7 adatoms.

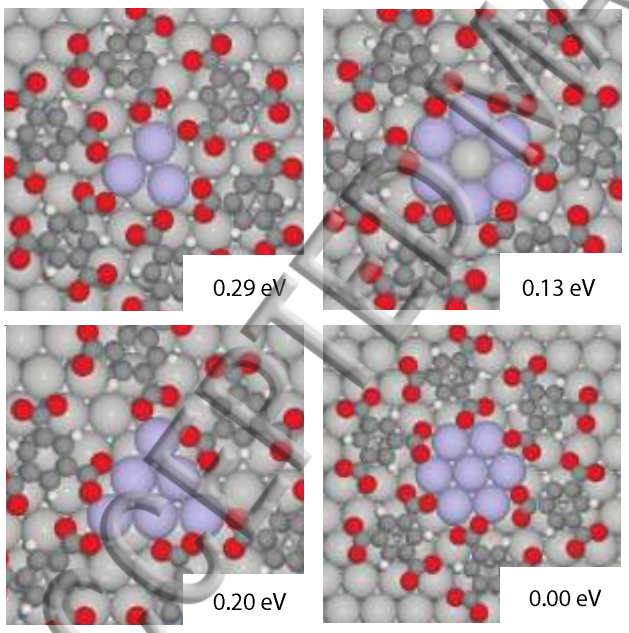

FIG 9 a) Isolated flowers with 3 adatoms and b-c) Structures with 6 adatoms compared with d) the structure with 7 adatoms. The energies are per molecule in the isolated flower on 4 layers of Ag, and include the cost of adatom formation. The adatoms are coloured darker for clarity.

Appendix D: Structures on gold

For comparison with the structure on gold we scaled the coordinates of the optimised structure on Ag to match the periodicity of gold (lattice constant 4.21Å with optB88-vdW, exp. 4.08Å[32]) and relaxed with the same convergence parameters as used on silver. This is compared to the calculated adsorption energies of isolated intact and dehydrogenated TMA in the adsorption sites that were found to be most favourable for the corresponding species on silver. The energies are compared in Figure 10, and illustrate that the dehydrogenation of TMA on Au(111) is very unfavourable. Surprisingly, the higher cohesive energy of Au compared with Ag (3.20eV vs. 2.67 eV as calculated with the optB88-vdW functional) only leads to a negligible energy difference in the formation energy of the adatom cluster (1.91eV for Ag and 1.94eV for Au). Note that since we have not investigated all adsorption sites for the isolated molecules the values are an upper bound.

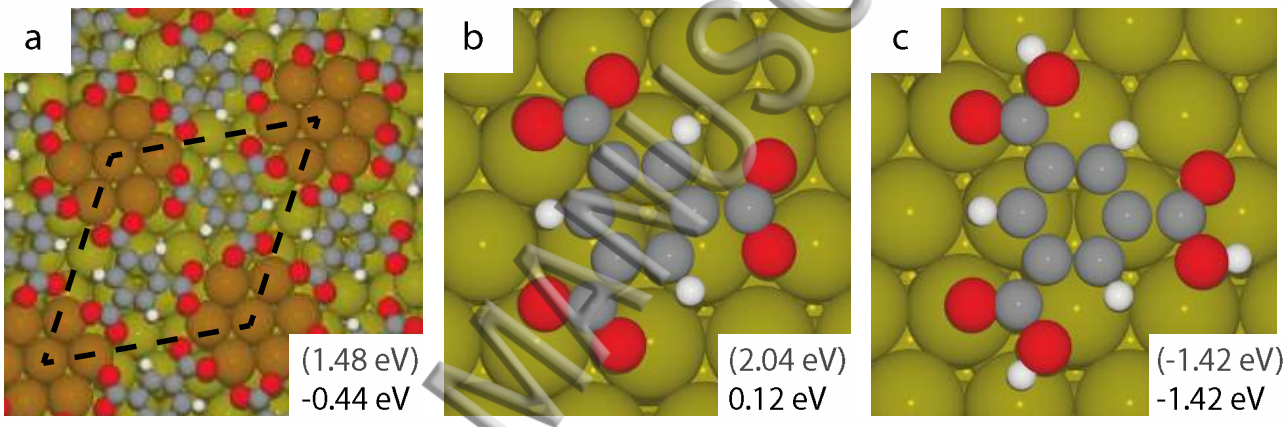

FIG 10: a) Metal-coordinated structure on Au(111) and b) isolated dehydrogenated molecule and c) isolated intact molecule. The free energies (black) and enthalpies (grey) per molecule are given in the lower right corner.

ACKNOWLEDGEMENTS

This work is supported by the Lundbeck Foundation, and the Danish Council for Independent Research.

REFERENCES

[1] L. Dong, Z. Gao, and N. Lin, Prog. Surf. Sci. **91**, 101 (2016).

[2] B.R. Cuenya, Thin Solid Films **518**, 3127 (2010).

[3] J. Lee, O.K. Farha, J. Roberts, K.A. Scheidt, S.T. Nguyen, and J.T. Hupp, Chem. Soc. Rev. **38**, 1450 (2009).

[4] S. Fabris, S. Stepanow, N. Lin, P. Gambardella, A. Dmitriev, J. Honolka, S. Baroni, and K. Kern, Nano Lett. **11**, 5414 (2011).

[5] A.P. Seitsonen, H. Spillmann, A. Dmitriev, S. Stepanow, N. Lin, K. Kern, and J. V Barth, J. Am. Chem. Soc. **128**, 5634 (2006).

[6] P. Gambardella, S. Stepanow, A. Dmitriev, J. Honolka, F.M.F. de Groot, M. Lingenfelder, S. Sen Gupta, D.D. Sarma, P. Bencok, S. Stanescu, S. Clair, S. Pons, N. Lin, A.P. Seitsonen, H. Brune, J. V Barth, and K. Kern, Nat. Mater. **8**, 189 (2009).

[7] K.H. Ernst, Phys. Status Solidi Basic Res. **249**, 2057 (2012).

[8] H. Spillmann, A. Dmitriev, Nian Lin, P. Messina, A. Johannes V. Barth, and K. Kern, J. Am. Chem. Soc. **125**, 10725 (2003).

[9] A. Dmitriev, H. Spillmann, M. Lingenfelder, Nian Lin, A. Johannes V. Barth, and K. Kern, Langmuir **20**, 4799 (2004).

[10] M. Ortega Lorenzo, C.J. Baddeley, C. Muryn, and R. Raval, Nature **404**, 376 (2000).

[11] P. Messina, A. Dmitriev, N. Lin, H. Spillmann, M. Abel, J. V. Barth, and K. Kern, J. Am. Chem. Soc. **124**, 14000 (2002).

[12] D. Payer, A. Comisso, A. Dmitriev, T. Strunskus, N. Lin, C. Wöll, A. DeVita, J. V. Barth, and K. Kern, Chem. - A Eur. J. **13**, 3900 (2007).

[13] N. Lin, D. Payer, A. Dmitriev, T. Strunskus, C. Wöll, J. V. Barth, and K. Kern, Angew. Chemie - Int. Ed. **44**, 1488 (2005).

[14] M.S. Baviloliaei and L. Diekhöner, Phys. Chem. Chem. Phys. **16**, 11265 (2014).

[15] J. Lipton-Duffin, M. Abyazisani, and J. MacLeod, Chem. Commun. **54**, 8316 (2018).

[16] H. Kong, L. Wang, Q. Tan, C. Zhang, Q. Sun, and W. Xu, Chem. Commun. **50**, 3242 (2014).

[17] F. Bebensee, K. Svane, C. Bombis, F. Masini, S. Klyatskaya, F. Besenbacher, M. Ruben, B. Hammer, and T.R. Linderoth, Angew. Chemie - Int. Ed. **53**, 12955 (2014).

[18] A. Shchyrba, C. Wäckerlin, J. Nowakowski, S. Nowakowska, J. Björk, S. Fatayer, J. Girovsky, T. Nijs, S.C. Martens, A. Kleibert, M. Stöhr, N. Ballav, T.A. Jung, and L.H. Gade, J. Am. Chem. Soc. **136**, 9355 (2014).

[19] N. Lin, A. Dmitriev, J. Weckesser, J. V. Barth, and K. Kern, Angew. Chemie - Int. Ed. **41**, 4779 (2002).

[20] J. Rodríguez-Fernández, K. Lauwaet, M.Á. Herranz, N. Martín, J.M. Gallego, R. Miranda, and R. Otero, J. Chem. Phys. **142**, 101930 (2015).

[21] Y.C. Xie, L. Tang, and Q. Guo, Phys. Rev. Lett. **111**, 1 (2013).

[22] Y.C. Xie, M. Rokni Fard, D. Kaya, D. Bao, R.E. Palmer, S. Du, and Q. Guo, J. Phys. Chem. C **120**, 10975 (2016).

[23] L. Schuller, V. Haapasilta, S. Kuhn, H. Pinto, R. Bechstein, A.S. Foster, and A. K??hnle, J. Phys. Chem. C **120**, 14730 (2016).

[24] K.-H. Chung, B.-G. Koo, H. Kim, J.K. Yoon, J. Kim, Y.-K. Kwon, S.-J. Kahng, J. Keon, and J. Kim, Phys. Chem. Chem. Phys. **14**, 7304 (2012).

[25] J. Park, K.Y. Kim, K.H. Chung, J.K. Yoon, H. Kim, S. Han, and S.J. Kahng, J. Phys. Chem. C **115**, 14834 (2011).

[26] J. Enkovaara, C. Rostgaard, J.J. Mortensen, J. Chen, M. Dułak, L. Ferrighi, J. Gavnholt, C. Glinsvad, V. Haikola, H. a Hansen, H.H. Kristoffersen, M. Kuisma, a H. Larsen, L. Lehtovaara, M. Ljungberg, O. Lopez-Acevedo, P.G. Moses, J. Ojanen, T. Olsen, V. Petzold, N. a Romero, J. Stausholm-Møller, M. Strange, G. a Tritsaris, M. Vanin, M. Walter, B. Hammer, H. Häkkinen, G.K.H. Madsen, R.M. Nieminen, J.K. Nørskov, M. Puska, T.T. Rantala, J. Schiøtz, K.S. Thygesen, and K.W. Jacobsen, J. Phys. Condens. Matter **22**, 253202 (2010).

[27] J.J. Mortensen, L.B. Hansen, and K.W. Jacobsen, Phys. Rev. B **71**, 035109 (2005).

[28] S.R. Bahn and K.W. Jacobsen, Comput. Sci. Eng. **4**, 56 (2002).

[29] J. Klimes, D.R. Bowler, and A. Michaelides, J. Phys. Condens. Matter **22**, 022201 (2010).

[30] Y. Zhao and D.G. Truhlar, J. Chem. Phys. **125**, (2006).

[31] M.N. Groves, G. Goubert, A.M.H. Rasmussen, Y. Dong, J.C. Lemay, V. Demers-Carpentier, P.H. McBreen, and B. Hammer, Surf. Sci. **629**, 48 (2014).

[32] C. Kittel, *Introduction to Solid State Physics* (John Wiley and Sons Inc., n.d.).

[33] A. Dmitriev, N. Lin, and J. Weckesser, J. Phys. Chem. B **106**, 6907 (2002).

[34] Y. Ye, W. Sun, Y. Wang, X. Shao, X. Xu, F. Cheng, J. Li, and K. Wu, J. Phys. Chem. C **111**, 10138 (2007).

[35] K. Morgenstern, G. Rosenfeld, E. Lægsgaard, F. Besenbacher, and G. Comsa, Phys. Rev. Lett. **80**, 556 (1998).

[36] P. Stoltze, J.Phys. Condens. Matter **6**, 9495 (1994).

[37] N. Lin, A. Dmitriev, J. Weckesser, J. V. Barth, and K. Kern, Angew. Chemie Int. Ed. **41**, 4779 (2002).

[38] K.L. Svane and B. Hammer, J. Chem. Phys. **141**, 174705 (2014).

[39] F. Bebensee, K. Svane, C. Bombis, F. Masini, S. Klyatskaya, F. Besenbacher, M. Ruben, B. Hammer, and T. Linderoth, Chem. Commun. **49**, 9308 (2013).

[40] L. Giovanelli, O. Ourdjini, M. Abel, R. Pawlak, J. Fujii, L. Porte, J.M. Themlin, and S. Clair, J. Phys. Chem. C **118**, 14899 (2014).

[41] P. Norby, R. Dinnebier, and A.N. Fitch, Inorg. Chem. **41**, 3628 (2002).

[42] K.L. Svane, T.R. Linderoth, and B. Hammer, J. Chem. Phys. **144**, 084708 (2016).

[43] R.F.W. Bader, *Atoms in Molecules: A Quantum Theory* (Oxford University Press, 1994).

a

20 nm

b

5 nm

c

3 nm

d

3 nm

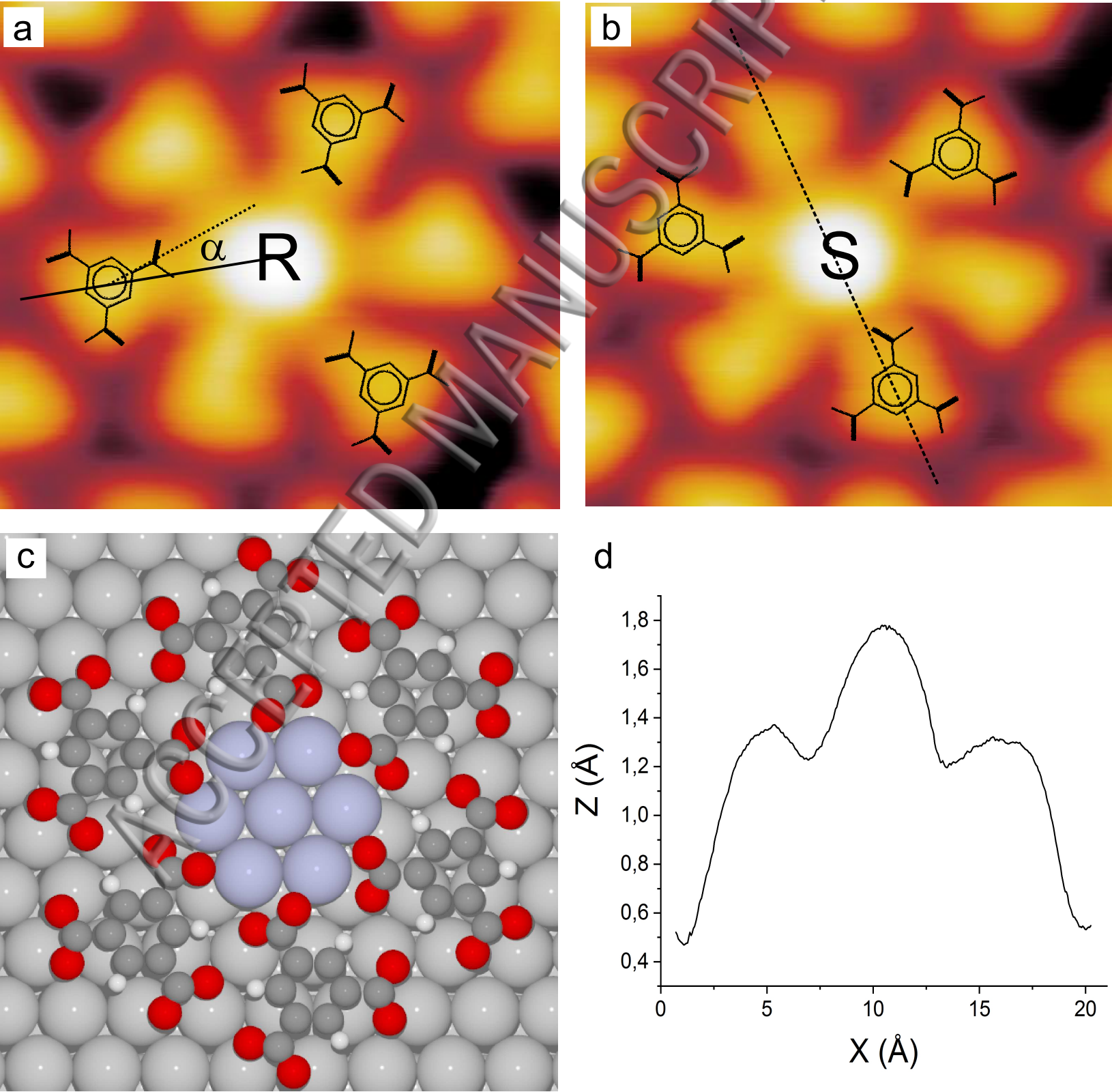

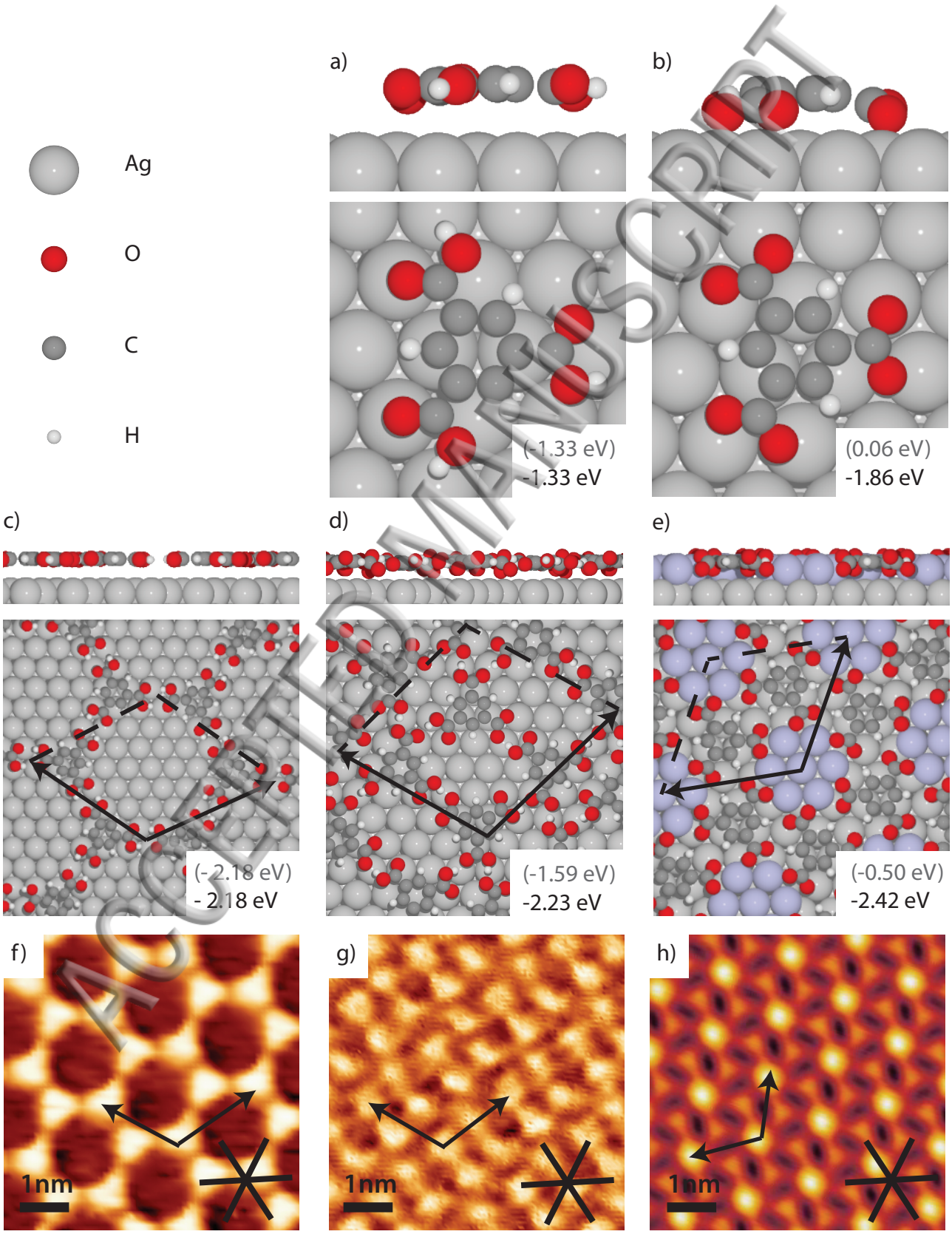

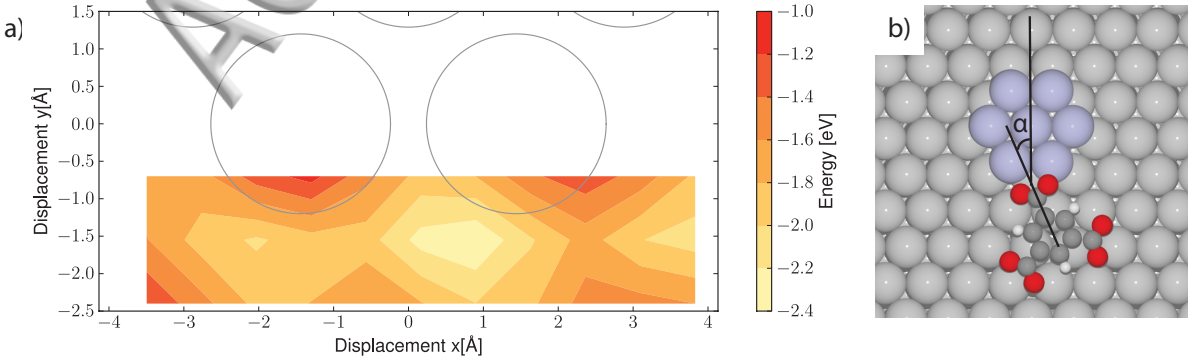
a)
Displacement y[Å]
Displacement x[Å]
Energy [eV]
b)
α

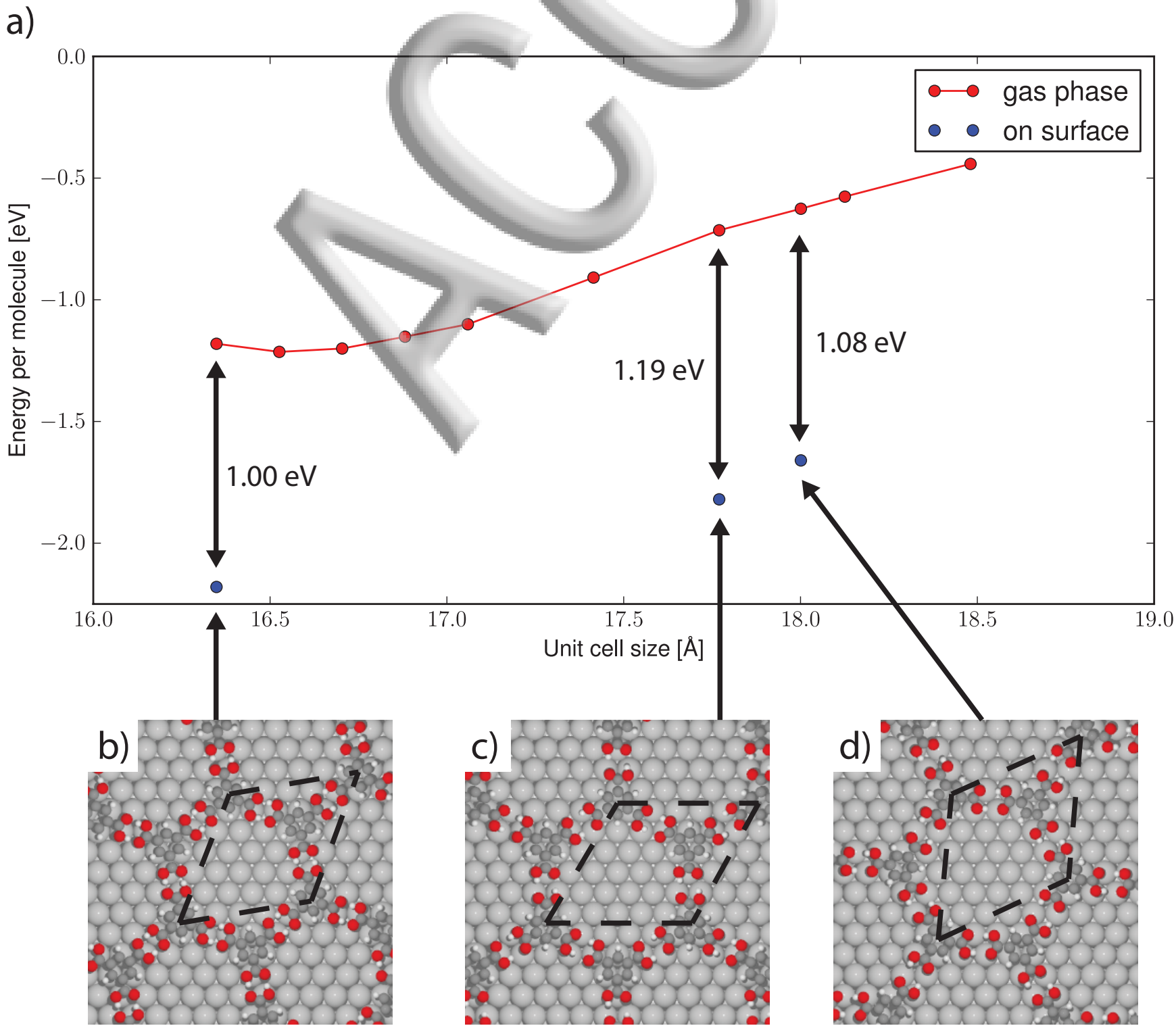
a)
0.0
−0.5
−1.0
−1.5
−2.0
Energy per molecule [eV]
gas phase
on surface
1.00 eV
1.19 eV
1.08 eV
16.0
16.5
17.0
17.5
18.0
18.5
19.0
Unit cell size [Å]
b)
c)
d)

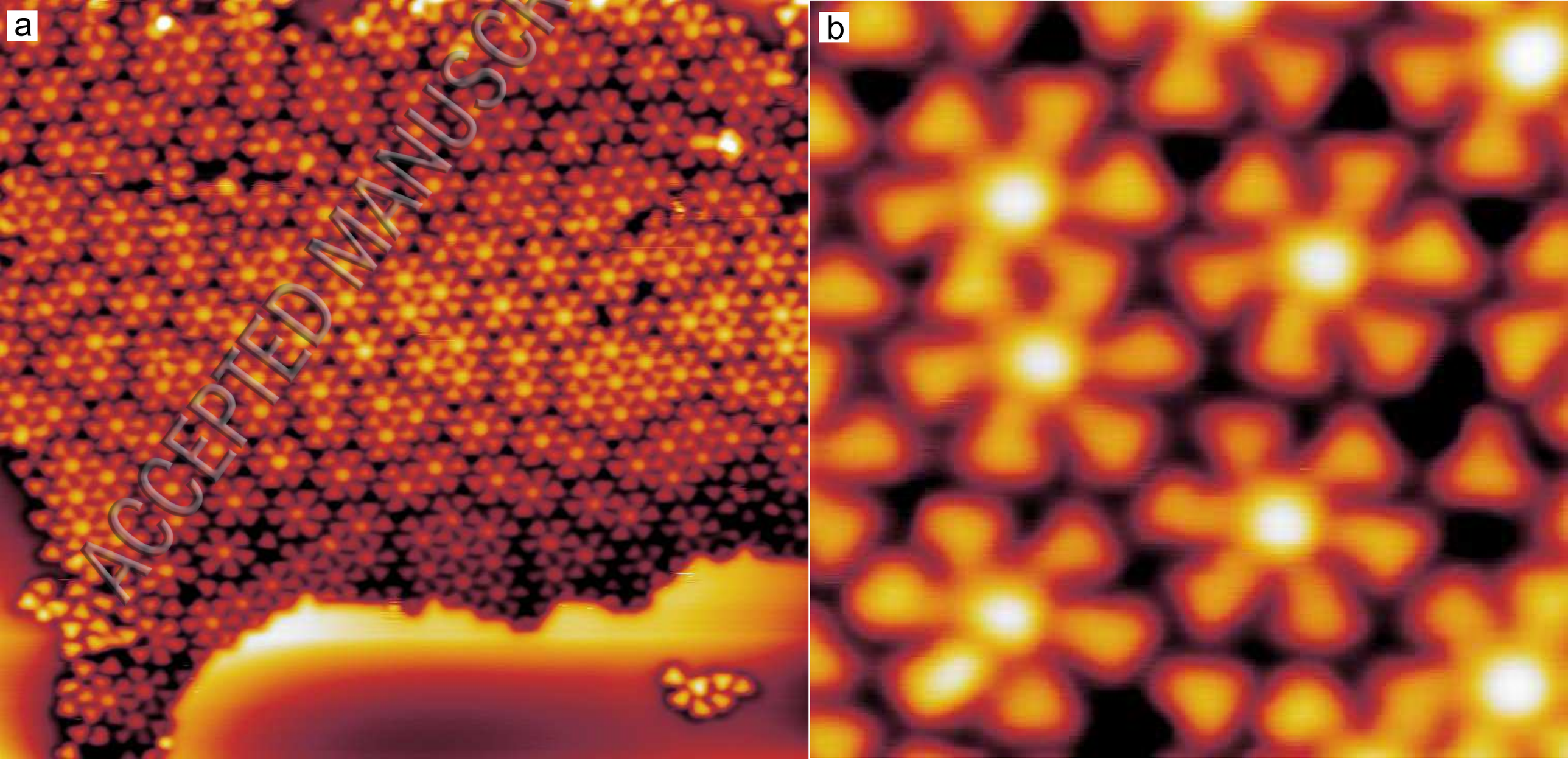

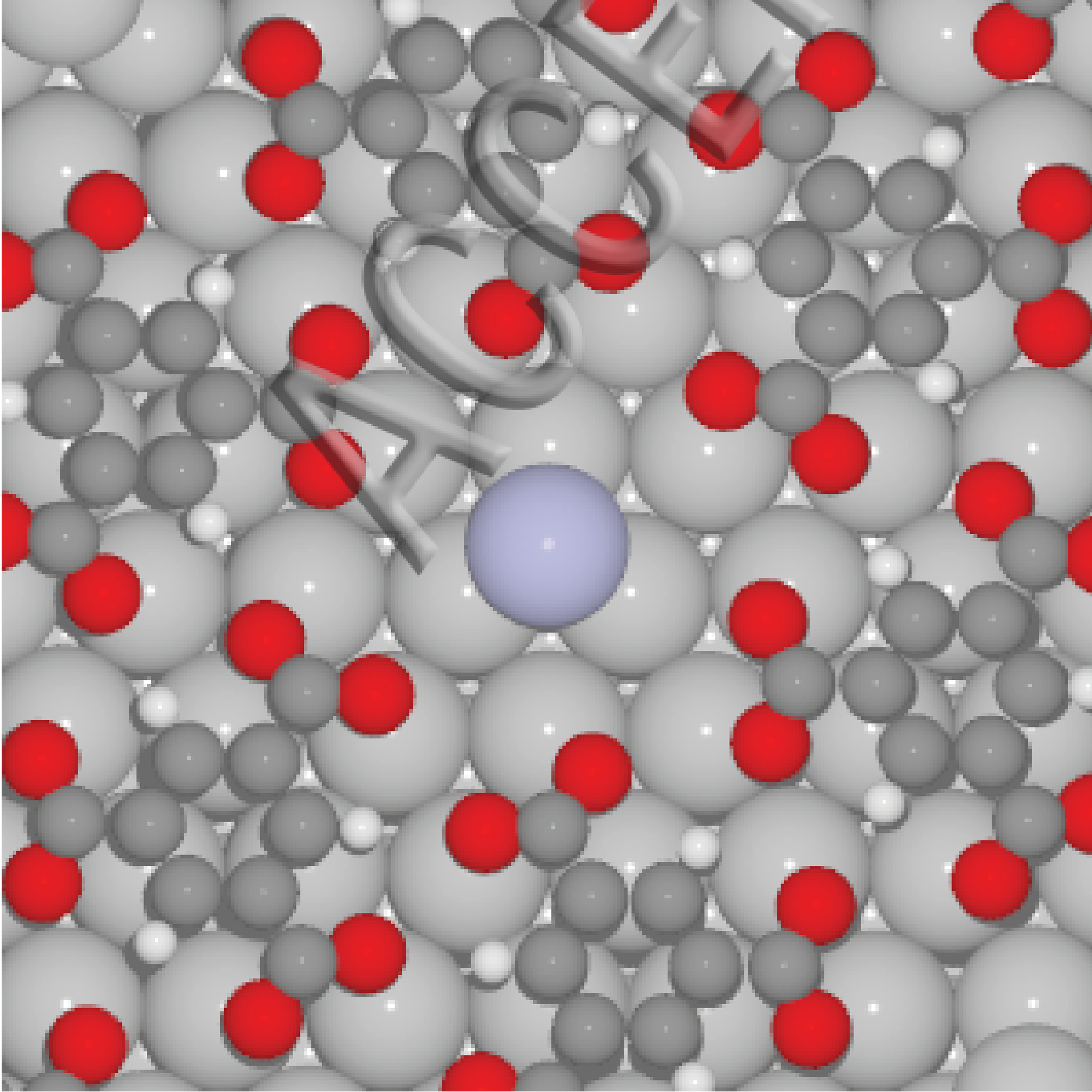

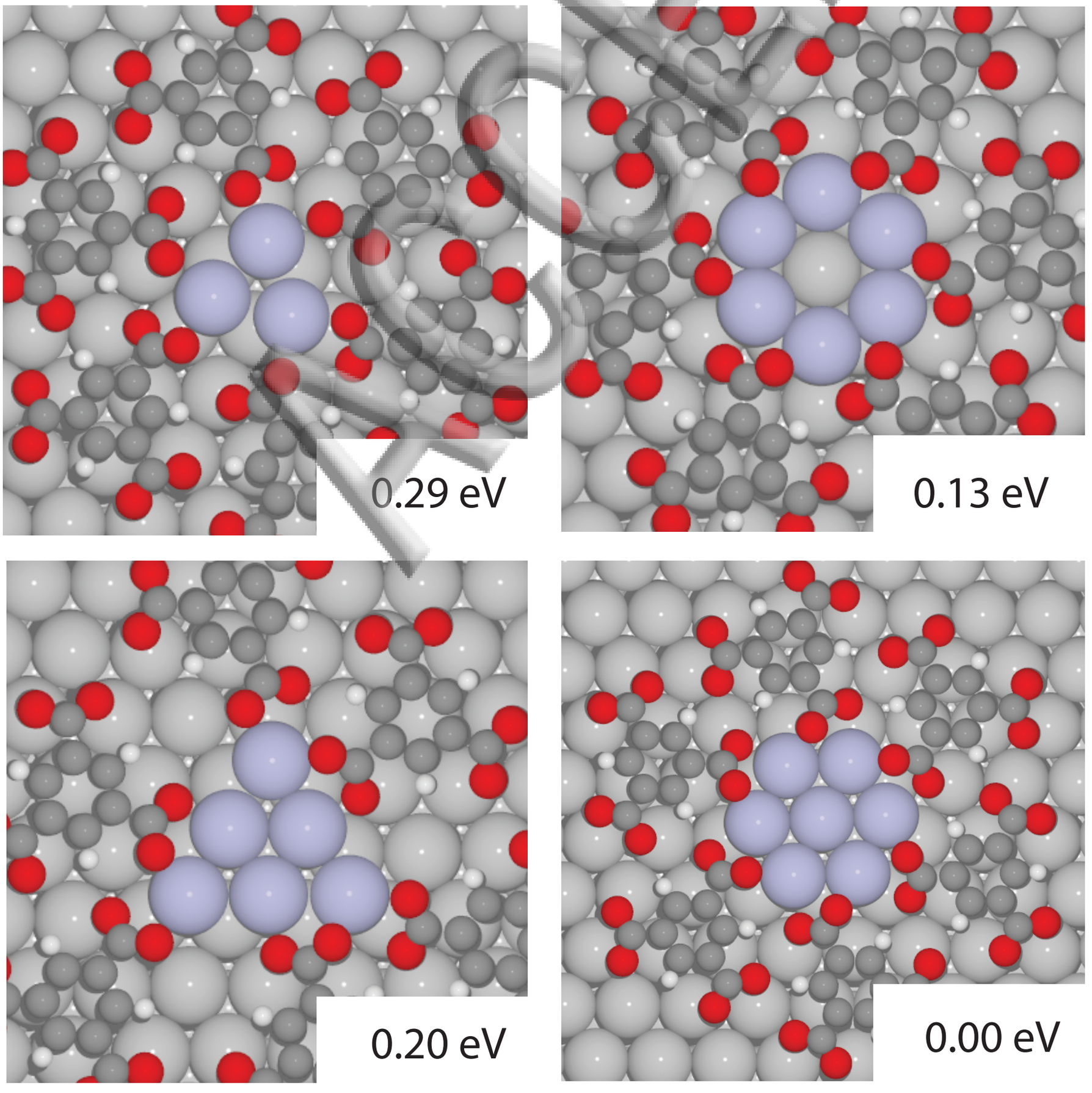
0.29 eV
0.13 eV
0.20 eV
0.00 eV

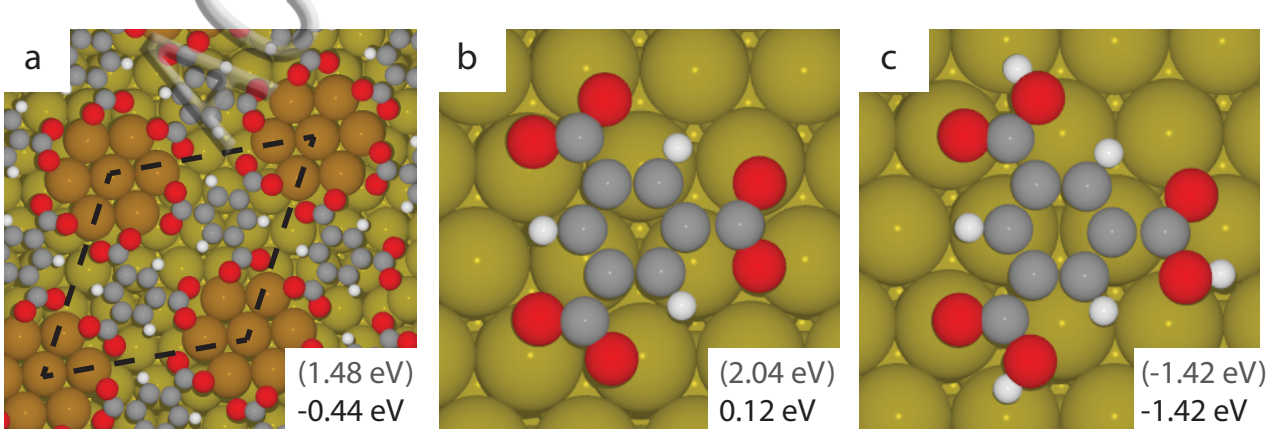
a
(1.48 eV)
-0.44 eV
b
(2.04 eV)
0.12 eV
c
(-1.42 eV)
-1.42 eV